MECHANICS

Original article
DOI: https://doi.org/10.18721/JPM.18312

A SOLUTION TO THE PROBLEM OF ELASTICITY CAUSED BY MASS TRANSPORT IN THE PRESENCE OF IMPERFECT CONTACTS AT THE INTERNAL INTERFACES OF A TWO-PHASE MATERIAL

K. P. Frolova[1]✉, *N. M. Bessonov*[1], *E. N. Vilchevskaya*[2]

[1] Institute for Problems in Mechanical Engineering RAS, St. Petersburg, Russia;

[2] Technical University of Berlin, Berlin, Germany

✉ fkp@ipme.ru

Abstract. The paper studies the influence of imperfect contacts (IC) at the phase interfaces of a micro-heterogeneous material on the macroscopic transport of impurity and the stress-strain state caused by its accumulation. Two types of IC are considered: segregation, which involves the accumulation of impurity that disrupts the continuity of concentration, and the formation of bypass paths for accelerated diffusion, which disrupts the continuity of the normal component of the flux. Modeling the coupled processes of mass transport and changes in the stress-strain state of the medium consists of two stages. In the first stage, the effective diffusion permeability of the material is determined using micromechanical methods. In the second stage, the macroscopic elasticity problem caused by mass transport is solved. The analysis is carried out using the example of a long cylinder, which is a two-phase material at the micro-level, consisting of a matrix and less permeable prolate spheroidal inhomogeneities with an arbitrary distribution of orientations.

Keywords: diffusion, elasticity due to mass transport, effective properties, imperfect contact, phase interface, two-phase material

Funding: The reported study was funded by Russian Science Foundation (Grant No. 23-79-01133 (https://rscf.ru/project/23-79-01133/).

Citation: Frolova K. P., Bessonov N. M., Vilchevskaya E. N., A solution to the problem of elasticity caused by mass transport in the presence of imperfect contacts at the internal interfaces of a two-phase material, St. Petersburg State Polytechnical University Journal. Physics and Mathematics. 18 (3) (2025) 141–155. DOI: https://doi.org/10.18721/JPM.18312

Научная статья
УДК 539.21
DOI: https://doi.org/10.18721/JPM.18312

РЕШЕНИЕ ЗАДАЧИ МАССОУПРУГОСТИ ПРИ НАЛИЧИИ НЕИДЕАЛЬНЫХ КОНТАКТОВ НА ВНУТРЕННИХ ГРАНИЦАХ ДВУХФАЗНОГО МАТЕРИАЛА

К. П. Фролова[1]✉, *Н. М. Бессонов*[1], *Е. Н. Вильчевская*[2]

[1] Институт проблем машиноведения РАН, Санкт-Петербург, Россия;

[2] Берлинский технический университет, г. Берлин, Германия

✉ fkp@ipme.ru

Аннотация. В работе исследовано влияние неидеальных контактов (НК) на границах раздела фаз неоднородного (на микроуровне) материала на транспорт примеси и на напряженно-деформированное состояние среды (на макроуровне), вызванное ее накоплением. Рассмотрены два типа НК: сегрегация (оседание примеси), когда нарушается непрерывность концентрации, и образование обходных путей ускоренной диффузии, когда нарушается непрерывность нормальной компоненты потока. Моделирование связанных процессов массопереноса и изменения напряженно-деформированного состояния среды включает два этапа. На первом определяется эффективная диффузионная проницаемость материала с помощью методов микромеханики. На втором этапе решается задача массоупругости на макроуровне. Анализ проведен на примере длинного цилиндра, представленного как двухфазный материал, состоящий из матрицы и менее проницаемых сфероидальных неоднородностей, имеющих вытянутую форму и произвольно распределенных по ориентациям. Показано, что тип НК и способ его учета могут оказывать существенное влияние на распределение примеси в образце и на величину внутреннего давления.

Ключевые слова: диффузия, массоупругость, эффективные свойства, неидеальный контакт, граница раздела фаз, двухфазный материал

Финансирование: Исследование выполнено при финансовой поддержке Российского научного фонда, грант № 01133-79-23 (https://rscf.ru/project/23-79-01133/).

Ссылка для цитирования: Фролова К. П., Бессонов Н. М., Вильчевская Е. Н. Решение задачи массоупругости при наличии неидеальных контактов на внутренних границах двухфазного материала // Научно-технические ведомости СПбГПУ. Физико-математические науки. 2025. Т. 3 № .18. С. 141–155. DOI: https://doi.org/10.18721/JPM.18312

Introduction

As more new materials are created and their range of applications expands, new challenges arise, associated with describing the state of objects under thermomechanical loads, taking into account the influence of various characteristics of the internal structure. Simulations of the behavior of materials that are inhomogeneous at the meso-level can be divided into two stages: at the first stage, effective properties are determined using micromechanical methods, and at the second stage, the problem is solved at the macro-level.

As a rule, calculations of the effective properties assume that the fields are continuous at the phase interfaces in the material [1]. However, this hypothesis may prove invalid in some cases. In particular, in the context of the problem on determining the diffusion properties, segregation (impurity deposition) [2] cannot be described if the concentration field is assumed to be continuous [3]. Cracking, grain refinement, etc., can lead to the formation of additional bypasses of accelerated diffusion [4], which, in turn, contradicts the assumption of continuity of the normal component of the flux.

Any disruption of field continuity means the presence of imperfect contact (IC) [5]. ICs of the above types have been taken into account in a number of studies describing various processes. For example, the diffusion process was considered in [6–8] taking into account segregation in a material consisting of a matrix and isolated inhomogeneities. The model introduced a parameter equal to the ratio of concentrations on the outer and inner sides of the phase interface (the segregation parameter). Thermal processes in two-phase materials containing isolated inhomogeneities were considered in [9–11] taking into account various types of imperfect contact. It was assumed that the inhomogeneities have a coating with extreme properties (it is an insulator or superconductor). We carried out generalization and comparison of different approaches to simulation of imperfect contacts in [12].

The presence of imperfect contacts that must be taken into account to determine the effective diffusion permeability can directly affect both the impurity distribution in the macroscopic sample and its stress–strain state, as the latter can change as a result of impurity accumulation. We analyzed the effect of segregation on diffusion and mass elasticity in [13]. Impurity deposition at the phase interface between matrix and inhomogeneity was modeled only by setting the segregation parameter.

This study focuses on analysis of the influence of two types of imperfect contacts (segregation and the formation of additional bypasses of accelerated diffusion). These contacts are investigated by different approaches: determining a jump in the field and considering an inhomogeneity with a thin coating of extreme properties.

The analysis is presented for a two-phase material consisting of a matrix and less conductive, arbitrarily oriented inhomogeneities shaped like prolate spheroids. This microstructure is typical, in particular, for polycrystals used in simulation of grains with inhomogeneities and grain boundaries with the matrix [7]. Hydrogen-assisted degradation is a major issue in polycrystals, as the accumulation of hydrogen leads to fracture of metals [14, 15].

Simulation stages

Coupled processes of mass transfer and change in the stress–strain state of the material in the presence of two types of imperfect contacts at the phase interface (segregation and formation of additional bypasses for accelerated diffusion) on a smaller scale is modeled in two stages. At the first stage, the effective diffusion permeability of the material is determined taking into account its internal structure; at the second stage, the coupled problem of mass transport and elasticity is solved, taking into account the macroscopic properties found.

To determine the effective diffusion permeability $\mathbf{D}^{eff}$, we limit ourselves to considering linear macroisotropic material, i.e.,

$$\mathbf{D}^{eff} = D^{eff}\mathbf{I}$$

($\mathbf{I}$ is a unit tensor); this material consists of an isotropic matrix with the permeability $\mathbf{D}_0 = D_0\mathbf{I}$ and isotropic inhomogeneities with permeability $\mathbf{D}_1 = D_1\mathbf{I}$, shaped as prolate spheroids with an arbitrary orientation distribution.

Consider different types of imperfect contacts at the phase interface. Segregation is modeled by taking into account the discontinuity of the concentration field c. The additional bypasses of accelerated diffusion are modeled by taking into account the normal component of the flux J_n.

We solve the initial boundary-value quasi-static problem of elasticity caused by mass transport for a long cylinder with radius r_0. We assume that stresses and strains arise in the cylinder solely due to accumulation of diffusing species with a constant concentration maintained on the lateral surface. We consider two cases: with and without taking into account the phenomenon of pressure-induced diffusion, where the pressure gradient gives rise to an additional diffusion flux.

Next, we present a mathematical formulation of the problem for each simulation stage, discussing the methods for solving it.

Determination of effective material properties

These properties of the material are obtained from the solution to the homogenization problem for a representative volume V, which is a material point of the continuum at the macro-level [9]. The macroscopic diffusion permeability tensor $\mathbf{D}^{eff}$ relates the volume-averaged flux $\mathbf{J}$ and the concentration gradient c, in accordance with classical Fick's law:

$$< \mathbf{J} >_V = -\mathbf{D}^{eff} \cdot < \nabla c >_V . \tag{1}$$

It is assumed that the conservation law is fulfilled at each point of the representative volume:

$$\nabla \cdot \mathbf{J}(\mathbf{x}) = 0, \tag{2}$$

where $\mathbf{x}$ is the radius vector, and the flux is linearly related to the concentration gradient by the formula

$$\mathbf{J}(\mathbf{x}) = -\mathbf{D}(\mathbf{x}) \cdot \nabla c(\mathbf{x}), \tag{3}$$

where $\mathbf{D}(\mathbf{x})$ is the diffusion permeability tensor of the material at point $\mathbf{x}$.

It is convenient to define a homogeneous Hill condition on the boundary Σ of the representative volume:

$$c(\mathbf{x})\big|_\Sigma = \mathbf{G}_0 \cdot \mathbf{x}. \tag{4}$$

The presence of imperfect contacts is taken into account either by setting the field jump at the interface between matrix (+) and the inhomogeneity (–), or by considering inhomogeneities with a thin coating with extreme properties. In the latter case, it is first assumed that the inhomogeneity is represented by confocal ellipsoids whose semi-axes b_1, b_2, b_3 and a_1, a_2, a_3 are related as

$$b_i^2 = a_i^2 + \xi \ (i = 1,2,3), \ \xi = \text{const},$$

while the properties of the layer D_s formed by two ellipsoids are finite.

Then the passage to the limit is carried out at $\xi \to 0$ and either at $D_s \to 0$, or at $D_s \to \infty$, depending on the type of imperfect contact [10, 11].

As a result, the presence of segregation can be taken into account in the model either by setting the parameter s_c such that the concentration jump is defined as

$$[c] = (s_c - 1)\, c(\mathbf{x})\big|_{\mathbf{x}\to\Gamma-}, \tag{5}$$

(Γ is the interface of the inhomogeneity with the external normal $\mathbf{n}_\Gamma$), or by setting the dimensionless parameter β of the equivalent surface resistance, expressed as follows for spheroidal inhomogeneities

$$\beta = \frac{1+2\gamma^2}{2\gamma S} \frac{D_1}{a^2} \lim_{\xi\to 0, D_s\to 0} \frac{\xi}{D_s}, \tag{6}$$

where γ is the ratio of the spheroid semi-axes, $\gamma = a_3/a$; S is the surface area of the spheroid divided by $(4/3)\pi a^2$.

Similarly, the formation of additional bypasses of accelerated diffusion is taken into account either by setting the parameter s_f,

$$[J_n] = (s_f - 1)\, \mathbf{n}_\Gamma \cdot \mathbf{J}(\mathbf{x})\big|_{\mathbf{x}\to\Gamma-}, \tag{7}$$

characterizing a jump in the normal component of the flux, or by setting a dimensionless equivalent surface permeability λ, which, in the case of spheroids, takes the form

$$\lambda = \frac{1+2\gamma^2}{2\gamma S} \frac{1}{D_1 a^2} \lim_{\xi\to 0, D_s\to \infty} \xi D_s. \tag{8}$$

The problem of determining the effective properties consists of two stages. At the first stage, the problem of isolated inhomogeneity in an infinite matrix is solved. At the second stage, a homogenization scheme is used to account for the presence of multiple inhomogeneities.

Based on the solution to the problem of isolated inhomogeneity, we can obtain an expression for the tensor characterizing the contribution of inhomogeneity to the required property [1].

The tensor **H** characterizing the contribution to the diffusion permeability can be obtained from the representation of the average flux as

$$<\mathbf{J}>_V = -\left(\mathbf{D}_0 + \frac{V_1}{V}\mathbf{H}\right)\cdot\mathbf{G}_0. \tag{9}$$

Expression (9) takes into account that the average concentration gradient does not depend on the microstructure and is completely determined by boundary condition (4):

$$<\nabla c>_V = \mathbf{G}_0.$$

The sum of the contribution tensors is a microstructural parameter that can be used to express the macroscopic characteristics of a material. Expressions for the tensors corresponding to the contributions of ellipsoidal and, in particular, spheroidal inhomogeneities were obtained and analyzed in [8–12]. The presence of various imperfect contacts was taken into account in two ways: by setting the field jump and by considering the inhomogeneity with a coating with extreme properties.

Let us give the final expressions for the contribution tensors of spheroids taking into account various factors:

$$\mathbf{H}^{s_c} = D_0\left[\frac{D_1 - s_c D_0}{f_0 D_1 + (1-f_0)s_c D_0}\boldsymbol{\theta} + \sum_{i=1}^{3}\frac{D_1 - s_c D_0}{(1-2f_0)D_1 + 2f_0 s_c D_0}\mathbf{nn}\right] \tag{10}$$

accounting for the discontinuity of the concentration field using the parameter s_c;

$$\mathbf{H}^{\beta} = D_0\left[\frac{D_1 - D_0 - f_0 D_0 \beta\frac{S}{\gamma}}{f_0 D_1 + (1-f_0)D_0 + (1-f_0)D_0\beta\frac{S}{\gamma}(f_0 - F_\theta)}\boldsymbol{\theta} + \right.$$
$$\left. + \frac{D_1 - D_0 - (1-2f_0)D_0\beta\frac{S}{\gamma}}{(1-2f_0)D_1 + 2f_0 D_0 + 2f_0 D_0 \beta\frac{S}{\gamma}(1-2f_0 - F_n)}\mathbf{nn}\right] \tag{11}$$

accounting for the discontinuity of the concentration field using the dimensionless equivalent surface resistance β;

$$\mathbf{H}^{s_f} = D_0\left[\frac{s_f D_1 - D_0}{f_0 s_f D_1 + D_0(1-f_0)}\boldsymbol{\theta} + \frac{s_f D_1 - D_0}{(1-2f_0)s_f D_1 + 2f_0 D_0}\mathbf{nn}\right] \tag{12}$$

accounting for the discontinuity of the normal component of the flux using the parameter s_f;

$$\mathbf{H}^{\lambda} = D_0\left[\frac{D_1 - D_0 + \lambda D_1\frac{S}{\gamma}(1-f_0)}{f_0 D_1 + (1-f_0)D_0 + f_0\lambda D_1\frac{S}{\gamma}(1-f_0+F_\theta)}\boldsymbol{\theta} + \right.$$
$$\left. + \frac{D_1 - D_0 + 2f_0\lambda D_1\frac{S}{\gamma}}{(1-2f_0)D_1 + 2f_0 D_0 + (1-2f_0)\lambda D_1\frac{S}{\gamma}(2f_0 + F_n)}nn\right] \tag{13}$$

accounting for the discontinuity of the normal component of the flux using the dimensionless equivalent surface diffusion permeability λ.

The following notations are used in Eqs. (10)–(13): **n** is the unit vector along the symmetry axis of the spheroid; $\boldsymbol{\theta} = \mathbf{I} - \mathbf{nn}$; F_n, F_θ are functions of the parameter γ for which the equalities hold true:

$$F_n = \frac{f_0\left(1+2\gamma^2\right)-\gamma^2}{1+2\gamma^2}, \; F_\theta = -2F_n,$$

where

$$f_0(\gamma) = \frac{1-g(\gamma)}{2\left(1-\gamma^{-2}\right)}, \; g = g(\gamma) = \begin{cases} \dfrac{1}{\gamma\sqrt{1-\gamma^2}}\arctan\dfrac{\sqrt{1-\gamma^2}}{\gamma}, \; \gamma \le 1 \\ \dfrac{1}{2\gamma\sqrt{\gamma^2-1}}\ln\left(\dfrac{\gamma+\sqrt{\gamma^2-1}}{\gamma-\sqrt{\gamma^2-1}}\right), \; \gamma \ge 1. \end{cases}$$

To determine the effective properties of a material with multiple inhomogeneities, we use the Mori–Tanaka method [1, 16], giving physically consistent results for both small and large volume fractions of inclusions. We analyzed this method along with several others for materials with imperfect contacts earlier in [8]. Let us outline the main points of the method and present the results for effective diffusion permeability.

Within the framework of the Mori–Tanaka method, inhomogeneities are treated as isolated and the interaction between them is taken into account by placing them in an effective field averaged over the matrix rather than in the initial field $\mathbf{G}_0$ satisfying expression (4):

$$\mathbf{G}^{eff} = \langle \nabla c \rangle_{V_0}. \tag{14}$$

The very presence of an imperfect contact as well as its type and the approach to account for it directly influence the effective field. Note that for the Mori–Tanaka method to be applied, we need to take into account the discontinuity of the concentration field/normal component of the flux at two stages: when we solve the problem of the isolated inhomogeneity and when we use the homogenization scheme, since the parameters responsible for imperfect contact appear not only in expressions for contribution tensors [8]. Indeed, taking into account various factors, the effective diffusion permeability of a material with spheroidal inhomogeneities is defined as follows in terms of the contribution tensors:

$$\mathbf{D}^{eff} = \mathbf{D}_0 + \frac{1}{V}\sum_i V_i \mathbf{H}_i^{s_c} \cdot \left[(1-p)\mathbf{I} + \left(\frac{1}{s_c}\mathbf{D}_1 - \mathbf{D}_0\right)^{-1} \cdot \frac{1}{V}\sum_i V_i \mathbf{H}_i^{s_c}\right]^{-1} \tag{15}$$

accounting for imperfect contact using the parameter s_c;

$$\mathbf{D}^{eff} = \mathbf{D}_0 + \frac{1}{V}\sum_i V_i \mathbf{H}_i^{\beta} \cdot \Bigg[(1-p)\mathbf{I} + \frac{1}{V}\sum_i V_i \times$$
$$\times \left(\frac{1+\beta\dfrac{S}{\gamma}f_0}{D_1 - D_0 - D_0\beta\dfrac{S}{\gamma}f_0} H_{11_i}^{\beta}\boldsymbol{\theta}_i + \frac{1+\beta\dfrac{S}{\gamma}\left(1-2f_0\right)}{D_1 - D_0 - D_0\beta\dfrac{S}{\gamma}\left(1-2f_0\right)} H_{33_i}^{\beta}\mathbf{n}_i\mathbf{n}_i \right)\Bigg]^{-1} \tag{16}$$

accounting for the imperfect contact using the parameter β, here the tensors corresponding to the contributions of individual inhomogeneities are represented in coordinate form as $\mathbf{H}^{\beta} = H_{11}^{\beta}\left(\mathbf{I} - \mathbf{nn}\right) + H_{33}^{\beta}\mathbf{nn}$;

$$\mathbf{D}^{eff} = \mathbf{D}_0 + \frac{1}{V}\sum_i V_i \mathbf{H}_i^{s_f} \cdot \left[(1-p)\mathbf{I} + \left(s_f \mathbf{D}_1 - \mathbf{D}_0\right)^{-1} \cdot \frac{1}{V}\sum_i V_i \mathbf{H}_i^{s_f} \right]^{-1} \tag{17}$$

accounting for imperfect contact using the parameter s_f;

$$\mathbf{D}^{eff} = \mathbf{D}_0 + \frac{1}{V}\sum_i V_i \mathbf{H}_i^{\lambda} \cdot \left[(1-p)\mathbf{I} + \frac{1}{V}\sum_i V_i \times \right.$$

$$\left. \times \left(\frac{1}{D_1 - D_0 + D_1 \lambda \frac{S}{\gamma}(1-f_0)} H_{11_i}^{\lambda} \boldsymbol{\theta}_i + \frac{1}{D_1 - D_0 + 2D_1 \lambda \frac{S}{\gamma} f_0} H_{33_i}^{\lambda} \mathbf{n}_i \mathbf{n}_i \right)_j \right]^{-1} \tag{18}$$

accounting for imperfect contact using the parameter λ.

In the case when the inhomogeneities have the same properties and the same shape (while their sizes may generally be different), the summation operation in expressions (15)–(18) can be replaced by averaging over the orientations of the inhomogeneities.

$$1/V \sum_i V_i \ldots = p\langle \ldots \rangle,$$

which is reduced to averaging the tensor $\boldsymbol{\theta}$ and the dyadic **nn** in expressions (10)–(13) for the contribution tensors.

Consequently, we obtain the following final formulas for calculating the effective diffusion permeability of macroisotropic material consisting of isotropic phases (taking into account the arbitrary orientation distribution of inhomogeneities and, accordingly, equality $\langle \mathbf{nn} \rangle = (1/3)\mathbf{I}$ holding true):

$$\frac{D^{eff}}{D_0} = 1 + \frac{pA_{s_c}}{(1-p) + \frac{pA_{s_c}}{(\alpha/s_c - 1)}}, \quad A_{s_c} = \frac{2\, H_{11}^{s_c}/D_0 + H_{33}^{s_c}/D_0}{3} \tag{19}$$

accounting for imperfect contact using the parameter s_c (the dimensionless parameter $\alpha = D_1/D_0$ is introduced here);

$$\frac{D^{eff}}{D_0} = 1 + \frac{pA_{\beta}}{(1-p) + pB_{\beta}}, \quad A_{\beta} = \frac{2\, H_{11}^{\beta}/D_0 + H_{33}^{\beta}/D_0}{3},$$

$$B_{\beta} = \frac{2}{3}\frac{1+\beta \frac{S}{\gamma} f_0}{\alpha - 1 - \beta \frac{S}{\gamma} f_0}\frac{H_{11}^{\beta}}{D_0} + \frac{1}{3}\frac{1+\beta \frac{S}{\gamma}(1-2f_0)}{\alpha - 1 - \beta \frac{S}{\gamma}(1-2f_0)}\frac{H_{33}^{\beta}}{D_0} \tag{20}$$

accounting for imperfect contact using the parameter β;

$$\frac{D^{eff}}{D_0} = 1 + \frac{pA_{s_f}}{(1-p) + \frac{pA_{s_f}}{(\alpha s_f - 1)}}, \quad A_{s_f} = \frac{2\, H_{11}^{s_f}/D_0 + H_{33}^{s_f}/D_0}{3} \tag{21}$$

accounting for imperfect contact using the parameter s_f;

$$\frac{D^{eff}}{D_0} = 1 + \frac{pA_\lambda}{(1-p) + pB_\lambda}, \; A = \frac{2\, H_{11}^{\lambda}/D_0 + H_{33}^{\lambda}/D_0}{3},$$
$$B_\lambda = \frac{2}{3}\frac{1}{\alpha - 1 + \alpha K \frac{S}{\gamma}(1 - f_0)}\frac{H_{11}^{\lambda}}{D_0} + \frac{1}{3}\frac{1}{\alpha - 1 + 2\alpha K \frac{S}{\gamma} f_0}\frac{H_{33}^{\lambda}}{D_0} \tag{22}$$

accounting for imperfect contact using the parameter λ.

Solution to coupled problem of mass transport and elasticity

Now let us describe the diffusion process at the macro-level. The diffusion equation has the following local form:

$$\frac{\partial c}{\partial t} = -\nabla \cdot \mathbf{J}, \tag{23}$$

where t is the time.

The diffusion flux **J** can generally be driven by both a concentration gradient c and a pressure gradient P (pressure-induced diffusion; $P = -\mathrm{tr}\sigma$, where σ is the stress tensor):

$$\mathbf{J} = -D^{eff}\left(\nabla c + Ac\nabla P\right), \tag{24}$$

where $A = M\alpha_V/(3\rho RT)$ (M is the molar mass, α_V is the volumetric coefficient of thermal expansion, ρ is the density, R is the universal gas constant, T is the temperature).

Along with the case when the flux is given by expression (24), let us consider classical Fick's law:

$$\mathbf{J} = -D^{eff}\nabla c. \tag{25}$$

The presence of imperfect contacts at the meso-level is taken into account here in the coefficient D^{eff}, determined from one of the formulas (19)–(22) depending on the type of imperfect contact and the model used.

The stress–strain state of the material satisfies the equilibrium equation

$$\nabla \cdot \boldsymbol{\sigma} = 0. \tag{26}$$

As a rule, the accumulation of diffusing species leads only to volumetric expansion of the material. In this case, the constitutive relations between stress and strain ε are given by the Duhamel–Neumann equations:

$$\boldsymbol{\sigma} = -P\mathbf{I} + 2\mu\,\mathrm{dev}\,\boldsymbol{\varepsilon}, \; P = -K\left(\mathrm{tr}\,\boldsymbol{\varepsilon} - \alpha_V\left(c - c_0\right)\right)\mathbf{I}, \tag{27}$$

where c_0 is the reference concentration; K and μ are the bulk modulus and the shear modulus, respectively.

Strains in linear material are defined in terms of the displacement gradient as $\boldsymbol{\varepsilon} = \left(\nabla \mathbf{u}\right)^s$.

Example problem for long cylinder. Now let us consider an initial boundary-value problem for a long cylinder. We write a system of equations in a cylindrical coordinate system (r,φ,z); the unit basis vectors are denoted, respectively, as $\mathbf{e}_r$, $\mathbf{e}_\varphi$, $\mathbf{e}_z$.

A constant concentration c_1 is maintained on the lateral surface of the cylinder, and this surface is free from loading:

$$c\big|_{r=r_0} = c_1, \; \mathbf{e}_r \cdot \boldsymbol{\sigma}\big|_{r=r_0} = 0. \tag{28}$$

The following conditions are satisfied in the center of the cylinder:

$$\left.\frac{\partial c}{\partial r}\right|_{r=0} = 0, \; \mathbf{u}\cdot\mathbf{e}_r\big|_{r=0} < \infty. \tag{29}$$

The following integral equilibrium condition holds true in accordance with Saint-Venant's principle and the plane section hypothesis:

$$\int_0^{r_0} \mathbf{e}_z \cdot \boldsymbol{\sigma} r dr = 0. \tag{30}$$

Assuming axial symmetry, the solution to the problem takes the following form:

$$\mathbf{u} = u_r(r)\mathbf{e}_r + u_z(z)\mathbf{e}_z, \ \frac{\partial u_z}{\partial z} = \varepsilon = \text{const}, \ c = c(r). \tag{31}$$

The initial concentration distribution is assumed to be zero:

$$c\big|_{t=0} = c_0 = 0. \tag{32}$$

In accordance with expression (27) and taking into account assumptions (31), the nonzero components of the stress tensor take the following form:

$$\begin{aligned}
\sigma_{rr} &= -P + \frac{4\mu}{3}\left[\frac{\partial u_r}{\partial r} - \frac{1}{2}\left(\frac{u_r}{r} + \varepsilon\right)\right], \\
\sigma_{\varphi\varphi} &= -P + \frac{4\mu}{3}\left[\frac{u_r}{r} - \frac{1}{2}\left(\varepsilon + \frac{\partial u_r}{\partial r}\right)\right], \\
\sigma_{zz} &= -P + \frac{4\mu}{3}\left[\varepsilon - \frac{1}{2}\left(\frac{\partial u_r}{\partial r} + \frac{u_r}{r}\right)\right],
\end{aligned} \tag{33}$$

and the pressure P takes the form

$$P = -K\left(\frac{\partial u_r}{\partial r} + \frac{u_r}{r} + \varepsilon - \alpha_V c\right). \tag{34}$$

Let us turn to the dimensionless formulation of the problem, introducing the following scales:
radius of the cylinder r_0 for the radial coordinate r and the radial displacement u_r;
quantity $4\mu/3$ for the components of the stress tensor σ_{ii} and pressure P;
concentration c_1 maintained on the lateral surface for the concentration c.
The scale for time t is denoted as T.

Then the final system of equations, supplemented by initial and boundary conditions, takes the following form (the notations are preserved for dimensionless quantities):

$$\begin{cases}
\dfrac{\partial}{\partial r}\left[\dfrac{\partial u_r}{\partial r} + \dfrac{u_r}{r} - P\right] = 0, \\
P = -k\left(\dfrac{\partial u_r}{\partial r} + \dfrac{u_r}{r} + \varepsilon - \alpha_V c\right), \\
u_r\big|_{r=0} < \infty, \quad \left(-P + \left[\dfrac{\partial u_r}{\partial r} - \dfrac{1}{2}\left(\dfrac{u_r}{r} + \varepsilon\right)\right]\right)\Bigg|_{r=1} = 0, \\
\displaystyle\int_0^1 \left(-P + \left[\varepsilon - \frac{1}{2}\left(\frac{\partial u_r}{\partial r} + \frac{u_r}{r}\right)\right]\right) r dr = 0, \\
r\dfrac{\partial c}{\partial t} = F\dfrac{\partial}{\partial r}\left[r\left(\dfrac{\partial c}{\partial r} + A_k c\dfrac{\partial P}{\partial r}\right)\right] \\
c\big|_{r=1} = 1, \quad \dfrac{\partial c}{\partial r}\Big|_{r=0} = 0, \quad c\Big|_{t=0} = 0,
\end{cases} \tag{35}$$

where the dimensionless coefficients $k = 3K/4\mu$, $A_k = 4\mu/3A$ are introduced; F is the diffusion Fourier number, $F = D^{eff}T/r_0^2$.

Note that the presence of imperfect contacts in the dimensionless formulation of the problem is taken into account only in the diffusion Fourier number, since it includes the effective diffusion permeability. For a fixed time scale and the same cylinder radius, varying the parameter F means varying D^{eff}.

System of equations (35) was solved numerically using the implicit finite difference method. A one-dimensional spatial mesh was introduced along the r axis, concentration and radial displacements were set in nodes, stresses (including pressure) and strains were set in cells.

Analysis of results

Consider the influence of imperfect contacts on the solution to the coupled problem of mass transport and elasticity. Let us consider several models in this case. First, let us find a solution with and without taking into account pressure-induced diffusion. Secondly, let us consider two types of imperfect contacts: I and II.

I. Segregation occurs.

II. Additional bypasses of accelerated diffusion arise in the material.

We use two approaches to account for imperfect contact within the framework of each model.

1. The field jump is defined as a ratio of the quantities from the outer and inner sides of inhomogeneity boundary.

2. An inhomogeneity with a thin coating of extreme properties is introduced.

Let us compare the results obtained with those for the case of perfect contacts at the matrix/inhomogeneity interface. To compare the approaches, let us express the parameters s_c and s_f in terms of the equivalent surface resistance β and permeability λ, respectively:

$$s_c = 1 + \beta, \; s_f = 1 + 2\lambda; \tag{36}$$

then both approaches to accounting for imperfect contacts produce the same results in the case of spherical inhomogeneities.

The analysis is carried out for the example of a material consisting of a matrix and arbitrarily oriented prolate spheroidal inhomogeneities with a ratio of semi-axis lengths $\gamma = 10$; we adopt the ratio of diffusion permeabilities $\alpha = D_1/D_0 = 0.2$.

Let us first present the results for effective properties of the material with imperfect contacts. The effect of segregation is illustrated in Fig. 1.

As can be seen from Fig. 1, the diffusion permeability decreases with an increase in the volume fraction of inhomogeneities p, while the presence of imperfect contact leads to a more pronounced change in the property (see Fig. 1,*a*). Fig. 1,*b* shows the dependences of effective permeability on parameter β at fixed volume fraction of inhomogeneities $p = 0.9$. It can be seen that the difference

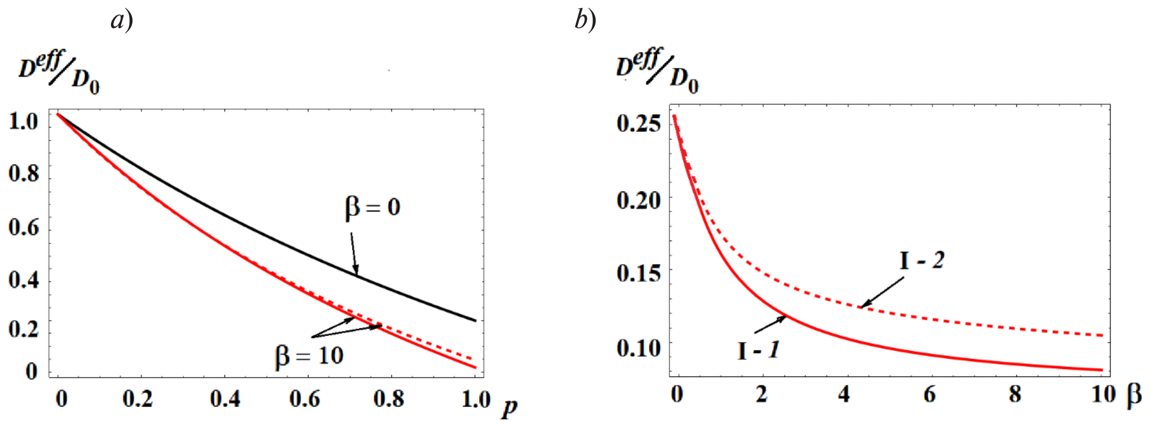

Fig. 1. Dependences of effective diffusion coefficient on volume fraction of inhomogeneities p for two values of parameter β (*a*) and on parameter β (*b*) for the case of segregation (I), simulated by approaches *1* and *2* (solid and dashed lines, respectively), see also the explanations in the text

between approaches to accounting for imperfect contact increases with increasing β. The difference remains insignificant with the selected characteristics of the structure.

The influence of the presence of bypasses for accelerated diffusion is shown in Fig. 2. Evidently, the presence of imperfect contact at the phase interface increases the diffusion permeability, compared with the case of its absence. Depending on the value of the parameter λ, the diffusion permeability can either decrease with an increase in the volume fraction of inhomogeneities, or increase, which is explained by the simultaneous influence of two competing factors, the presence of less conductive inhomogeneities in the matrix and bypasses of accelerated diffusion. Evidently, an increase in the parameter λ entails an increase in the difference between approaches to accounting for imperfect contact.

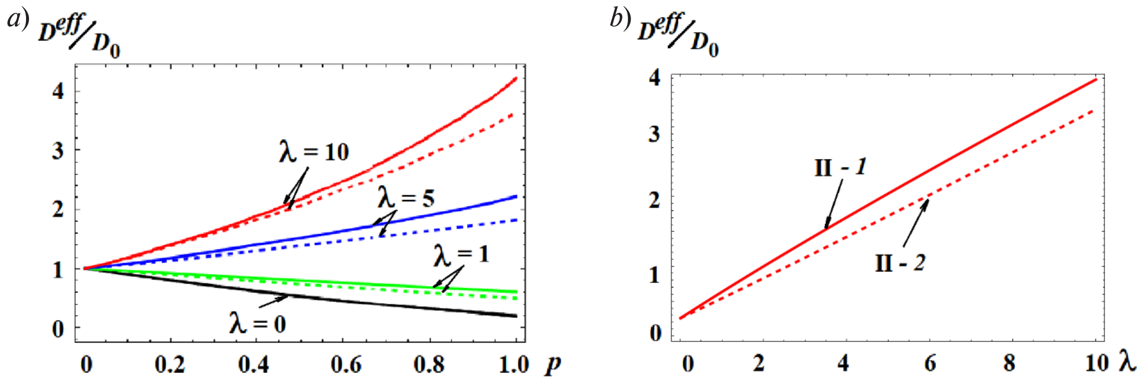

Fig. 2. Dependences of effective diffusion coefficient on volume fraction of inhomogeneities p at 4 values of parameter λ (*a*) and parameter λ (*b*) for the case of bypasses for accelerated diffusion (II), simulated by approaches *1* and *2* (solid and dashed lines, respectively), see also the explanations in the text

We solve the coupled problem of mass transport and elasticity with the following parameter values: $k = 1.6$, $A = 49.3$, $\alpha_V = 4.5\cdot10^{-6}$ (typical parameters for aluminum). The presence of imperfect contacts influences the value of the effective diffusion permeability and, consequently, the diffusion Fourier number F. Consider the values of D^{eff}/D_0 obtained at $p = 0.9$ and, depending on the type of imperfect contact, at $\beta = 10$ or $\lambda = 10$ (see column 3 in Table). Note that the ratios of the diffusion Fourier numbers corresponding to different values of the effective diffusion permeability are more important for analysis than the absolute values of F. We introduce the notation F_0

Table

Diffusion characteristics of material: calculation results

Model		Parameter value	
IC type	Approach to accounting for IC	D^{eff}/D_0	F_i
Without accounting for IC		0.26	$F_0 = 2.25\cdot10^{-4}$
I	*1*	0.08	$F_1 = 0.3\ F_0$
	2	0.10	$F_2 = 0.4\ F_0$
II	*1*	3.68	$F_3 = 14.2\ F_0$
	2	3.25	$F_4 = 12.5\ F_0$

Notations: D^{eff}/D_0 is the dimensionless effective diffusion permeability; F_i is the diffusion Fourier number; IC is the imperfect contact. The numbers I, II, *1*, *2* are explained in the text.

Note. The calculations were carried out for the material consisting of a matrix and arbitrarily oriented, prolate spheroidal inhomogeneities with a ratio of semi-axis lengths $\gamma = 10$.

for the Fourier number corresponding to the value of D^{eff}/D_0 obtained without taking into account imperfect contacts ($s_c = s_f = 1$, $\beta = \lambda = 0$). The value of F_0 is calculated at $D^{eff} = 1\cdot10^{-12}$ m²/s (typical parameter for aluminum), $r_0 = 0.004$ m, $T = 3600$ s = 1 h. The values of the diffusion Fourier number are given in Table (last column).

The concentration profiles and pressure dependences on the radius (cylindrical coordinate system) at different values of diffusion Fourier number at time $t = 100$ are shown in Fig. 3. Note that the results obtained without and with taking into account pressure-induced diffusion coincided with the given material parameters (the value of parameter A_k is small, so the pressure gradient multiplied by it turns out to be much smaller than the concentration gradient).

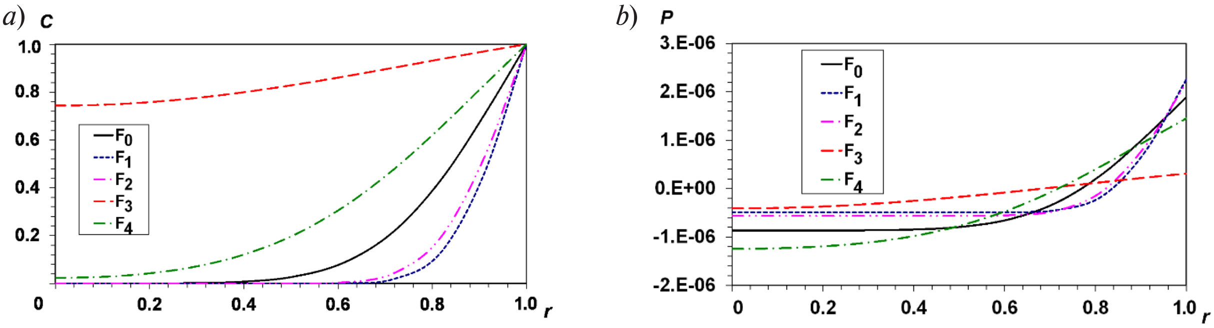

Fig. 3. Dependences of concentration (*a*) and pressure (*b*) on radius (coordinate along the polar axis) at different values of diffusion Fourier number (see Table) at time $t = 100$

Fig. 3 shows that the presence of imperfect contacts and the approach to accounting for them for has a significant influence on the concentration of diffusing species in the material and on its distribution. In particular, the presence of segregation for which a decrease in the diffusion rate is observed can considerably reduce the concentration of impurities in the material. The concentration gradient increases, which leads to more pronounced pressure drops. Such a variation in pressure, in turn, can be critical in problems of hydrogen degradation where local characteristics are important. The presence of bypasses for accelerated diffusion can lead to a significant increase in the concentration in the material, directly influencing its behavior in case of aggressive environments. The approach where the field jump is set as the ratio of the field values from the outer and inner sides of the inhomogeneity interface (both in the case of segregation and in the case of additional bypasses of accelerated diffusion) affects the result to a greater extent. The difference between models II-*1* and II-*2* used to simulate the discontinuity of the normal component of the flux is particularly significant.

The effect of pressure-induced diffusion was studied separately and is shown in Fig. 4. This effect occurs at higher values of the thermal expansion coefficient than the characteristic value for aluminum. In particular, the graphs in Fig. 4 are plotted for $\alpha_V = 0.2$. For clarity, the figure

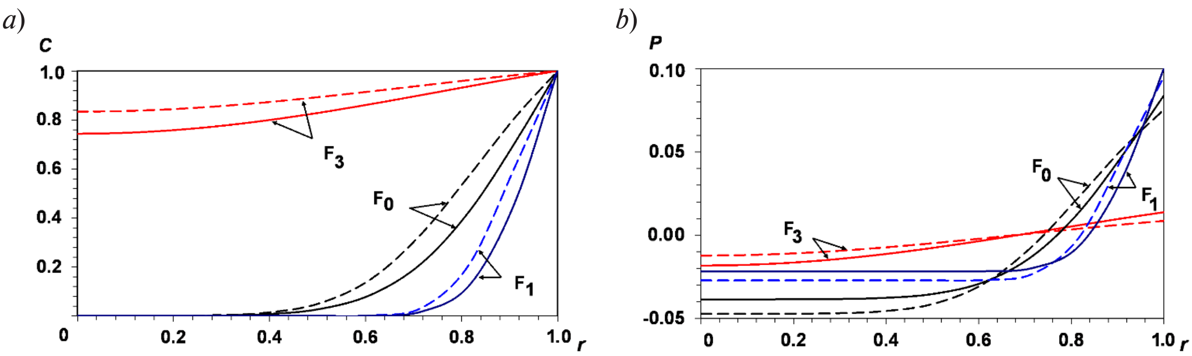

Fig. 4. Dependences of concentration (*a*) and pressure (*b*) of diffusing species on radius (coordinate along the polar axis) at different values of diffusion Fourier number (see Table), taking into account (dashed lines) and without taking into account (solid lines) pressure-induced diffusion

shows the results obtained at three values of F_0 from Table: at the value obtained without taking into account imperfect contacts as well as at the maximum and minimum values from the considered range. Fig. 4 shows that the presence of pressure-induced diffusion leads to an increase in the concentration of the diffusing species in the material, a decrease in both the concentration gradient and the pressure difference in all cases.

Thus, the presence, type, and approach to accounting for imperfect contacts influences the distribution of diffusing species in the material and its stress–strain state.

Conclusion

We obtained a solution to the coupled problem (in particular, to the one-way coupled problem) of diffusion and elasticity, describing the material's elastic behavior due to impurity accumulation taking into account the presence of imperfect contacts at the phase interface. Two types of imperfect contacts were considered: the presence of segregation (leading to discontinuity of the concentration field) and the presence of additional bypasses of accelerated diffusion (leading to discontinuity of the normal component of the flux). Each type of imperfect contact was taken into account within the framework of two approaches: by setting the ratio of the field magnitudes from the outer and inner sides of the inhomogeneity interface and by considering an inhomogeneity with a thin coating of extreme properties.

The microstructure was taken into account at the stage when the effective properties of the material were determined by the Mori–Tanaka homogenization method based on tensors describing the contributions to diffusion permeability.

The analysis was carried out for an axisymmetric sample made of two-phase material with arbitrarily oriented prolate spheroidal inhomogeneities characterized by lower diffusion permeability than the matrix.

It was established that the type of imperfect contact and the approach to accounting for it can have a significant effect on the distribution of impurities in the sample and on the internal pressure. This can be crucial, for example, in the case of saturation of metals with harmful impurities.

Thus, to improve the accuracy of stress–strain analysis, it is necessary to take into account the specifics of impurity transport and the presence of defects, so that the assumption of continuity of fields at the phase interfaces may have to be consequently abandoned.

REFERENCES

1. **Kachanov M., Sevostianov I.,** Micromechanics of materials, with applications (Book Ser. "Solid Mechanics and its Applications". Vol. 249), Springer, Berlin, Germany, 2018.

2. **Zhang X, Qiao L, Zhang H, Wang P.,** Influence of impurity gas seeding into deuterium plasma on the surface modification, sputtering erosion and deuterium retention in W and W-La_2O_3 alloy, Int. J. Hydr. Energy. 48 (6) (2023) 2075–2089.

3. **Zhang Y., Liu L.,** On diffusion in heterogeneous media, Am. J. Sci. 312 (9) (2012) 1028–1047.

4. **Chepak-Gizbrekht M. V., Knyazeva A. G.,** Two-dimensional model of grain boundary diffusion and oxidation, PNPU Mechanics Bulletin. (1) (2022) 156–166 (in Russian)

5. **Pham D. C., Nguyen T. K.,** General imperfect interface model for spherical–circular inclusion composites, Acta Mech. 235 (4) (2024) 2211–2229.

6. **Belova I. V., Murch G. E.,** Calculation of the effective conductivity and diffusivity in composite solid electrolytes, J. Phys. Chem. Solids. 66 (5) (2005) 722–728.

7. **Knyazeva A. G., Grabovetskaya G. P., Mishin I. P., Sevostianov I.,** On the micromechanical modelling of the effective diffusion coefficient of a polycrystalline material, Philos. Mag. 95 (19) (2015) 2046–2066.

8. **Frolova K. P., Vilchevskaya E. N.,** Effective diffusivity of transversely isotropic material with embedded pores, Mater. Phys. Mech. 47 (6) (2021) 937–950.

9. **Markov K. Z.,** Elementary micromechanics of heterogeneous media. Heterogeneous media: micromechanics modeling methods and simulations, Birkhдuser, Boston, MA, USA, 2000.

10. **Levin V., Markov M.,** Effective thermal conductivity of micro-inhomogeneous media containing imperfectly bonded ellipsoidal inclusions, Int. J. Eng. Sci. 109 (Dec) (2016) 202–215.

11. **Markov M., Levin V., Markova I.,** Determination of effective electromagnetic parameters of concentrated suspensions of ellipsoidal particles using Generalized Differential Effective Medium approximation, Phys. A: Stat. 492 (15 Febr) (2018) 113–122.

12. **Frolova K. P., Vilchevskaya E. N.,** Comparison of approaches to accounting for imperfect contacts when determining the effective permeability of material, St. Petersburg Polytechnical State University Journal. Physics and Mathematics. 16 (4) (2023) 146–159 (in Russian).

13. **Frolova K. P., Bessonov N. M., Vilchevskaya E. N.,** Diffusion in media with spheroidal pores, In book: V. A. Polyanskiy, A. K. Belyaev (Eds.). Mechanics and Control of Solids and Structures (Book Series: Advanced Structures Materials. Vol. 164), Springer Int. Publ., Cham, Switzerland (2022) 209–225.

14. **Sun Y., Cheng Y. F.,** Hydrogen-induced degradation of high-strength steel pipeline welds: A critical review, Eng. Fail. Anal. 133 (March) (2022) 105985.

15. **Sedova Y. S., Polyanskiy V. A., Belyaev A. K., Yakovlev Y. A.,** Modeling the skin effect, associated with hydrogen charging of samples, within the framework of the HEDE mechanism of cracking, Mater. Phys. Mech. 51 (6) (2023) 152–159.

16. **Mori T., Tanaka K.,** Average stress in matrix and average elastic energy of materials with misfitting inclusions, Acta Metall. 21 (5) (1973) 571–574.

СПИСОК ЛИТЕРАТУРЫ

1. **Kachanov M., Sevostianov I.** Micromechanics of materials, with applications (Book Series “Solid Mechanics and its Applications”. Vol. 249). Berlin, Germany: Springer, 2018. 712 p.

2. **Zhang X, Qiao L, Zhang H, Wang P.** Influence of impurity gas seeding into deuterium plasma on the surface modification, sputtering erosion and deuterium retention in W and W-La_2O_3 alloy // International Journal of Hydrogen Energy. 2023. Vol. 48. No. 6. Pp. 2075–2089.

3. **Zhang Y., Liu L.** On diffusion in heterogeneous media // American Journal of Science. 2012. Vol. 312. No. 9. Pp. 1028–1047.

4. **Чепак-Гизбрехт М. В., Князева А. Г.** Двумерная модель зернограничной диффузии и окисления // Вестник Пермского национального исследовательского политехнического университета. Механика. 2022. № 1. С. 156–166.

5. **Pham D. C., Nguyen T. K.** General imperfect interface model for spherical–circular inclusion composites // Acta Mechanica. 2024. Vol. 235. No. 4. Pp. 2211–2229.

6. **Belova I. V., Murch G. E.** Calculation of the effective conductivity and diffusivity in composite solid electrolytes // Journal of Physics and Chemistry of Solids. 2005. Vol. 66. No. 5. Pp. 722–728.

7. **Knyazeva A. G., Grabovetskaya G. P., Mishin I. P., Sevostianov I.** On the micromechanical modelling of the effective diffusion coefficient of a polycrystalline material // Philosophical Magazine. 2015. Vol. 95. No. 19. Pp. 2046–2066.

8. **Frolova K. P., Vilchevskaya E. N.** Effective diffusivity of transversely isotropic material with embedded pores // Materials Physics and Mechanics. 2021. Vol. 47. No. 6. Pp. 937–950.

9. **Markov K. Z.** Elementary micromechanics of heterogeneous media. Heterogeneous media: micromechanics modeling methods and simulations. Boston, USA: Birkhдuser, MA, 2000. 162 p.

10. **Levin V., Markov M.** Effective thermal conductivity of micro-inhomogeneous media containing imperfectly bonded ellipsoidal inclusions // International Journal of Engineering Science. 2016. Vol. 109. December. Pp. 202–215.

11. **Markov M., Levin V., Markova I**. Determination of effective electromagnetic parameters of concentrated suspensions of ellipsoidal particles using Generalized Differential Effective Medium approximation // Physica A: Statistical Mechanics and its Applications. 2018. Vol. 492. 15 February. Pp. 113–122.

12. **Фролова К. П., Вильчевская Е. Н.** Сравнение подходов к учету неидеальных контактов при определении эффективной проницаемости материала // Научно-технические ведомости Санкт-Петербургского государственного политехнического университета. Физико-математические науки. 2023. Т. 16. №. 4. С. 146–159.

13. **Frolova K. P., Bessonov N. M., Vilchevskaya E. N.** Diffusion in media with spheroidal pores // V. A. Polyanskiy, A. K. Belyaev (Eds.). Mechanics and Control of Solids and Structures (Book Series: Advanced Structures Materials. Vol. 164). Cham, Switzerland: Springer International Publishing, 2022. Pp. 209–225.

14. **Sun Y., Cheng Y. F.** Hydrogen-induced degradation of high-strength steel pipeline welds: A critical review // Engineering Failure Analysis. 2022. Vol. 133. March. P. 105985.

15. **Sedova Y. S., Polyanskiy V. A., Belyaev A. K., Yakovlev Y. A.** Modeling the skin effect, associated with hydrogen charging of samples, within the framework of the HEDE mechanism of cracking // Materials Physics and Mechanics. 2023. Vol. 51. No. 6. Pp. 152–159.
16. **Mori T., Tanaka K.** Average stress in matrix and average elastic energy of materials with misfitting inclusions // Acta Metallurgica. 1973. Vol. 21. No. 5. Pp. 571–574.

THE AUTHORS

FROLOVA Ksenia P.
Institute for Problems in Mechanical Engineering of RAS
61 Bolshoi Ave. V. O., St. Petersburg, 199178, Russia
fkp@ipme.ru
ORCID: 0000-0003-0376-4463

BESSONOV Nikolay M.
Institute for Problems in Mechanical Engineering of RAS
61 Bolshoi Ave. V. O., St. Petersburg, 199178, Russia
nickbessonov1@gmail.com
ORCID: 0000-0001-6462-5980

VILCHEVSKAYA Elena N.
Technical University of Berlin, Germany
Straße des 17. Juni 135 10623, Berlin
vilchevska@gmail.com
ORCID: 0000-0002-5173-3218

СВЕДЕНИЯ ОБ АВТОРАХ

ФРОЛОВА Ксения Петровна – *кандидат физико-математических наук, старший научный сотрудник лаборатории прикладных исследований*
Института проблем машиноведения РАН.
199178, Россия, г. Санкт-Петербург, Большой проспект В. О., 61.
fkp@ipme.ru
ORCID: 0000-0003-0376-4463

БЕССОНОВ Николай Михайлович – *доктор физико-математических наук, главный научный сотрудник лаборатории микромеханики материалов Института проблем машиноведения РАН.*
199178, Россия, г. Санкт-Петербург, Большой проспект В. О., 61.
nickbessonov1@gmail.com
ORCID: 0000-0001-6462-5980

ВИЛЬЧЕВСКАЯ Елена Никитична – *доктор физико-математических наук, приглашенный специалист Берлинского технического университета.*
Straße des 17. Juni 135 10623, Berlin
vilchevska@gmail.com
ORCID: 0000-0002-5173-3218

Received 28.03.2025. Approved after reviewing 17.04.2025. Accepted 17.04.2025.
Статья поступила в редакцию 28.03.2025. Одобрена после рецензирования 17.04.2025. Принята 17.04.2025.